ENVIRONMENT ASSISTED FRACTURE OF METALLIC GLASSES

T. K. G. Namboodhiri

Department of Metallurgical Engineering, Banaras Hindu University, Varanasi-221005, India

ABSTRACT

Hydrogen embrittlement and stress corrosion cracking of three metal-metalloid glasses based on iron and nickel were studied in sulfuric and hydrochloric acid media using slow strain rate tensile testing and scanning electron microscopy. All the three alloys were found to be susceptible to hydrogen embrittlement which results in a drastic reduction in fracture stress and a brittle fracture morphology. Only one of the alloys was found to be susceptible to stress corrosion cracking. From fractographic observations of voids at the hydrogen embrittled fracture surfaces it is suggested that hydrogen may collect at localized shear bands and cause the premature brittle failure of these materials.

KEYWORDS

Hydrogen embrittlement; stress corrosion cracking; metal-metalloid glasses; corrosion resistance; fracture morphology.

INTRODUCTION

Metallic glasses are materials with exceptional magnetic and mechanical properties coupled with extremely high corrosion resistance (Masumoto, 1981). The soft magnetic properties of several iron, nickel and cobalt base metal-metalloid glasses are now commercially exploited in transformer cores, tape heads, and magnetic shields. Chromium containing metallic glasses have remarkable corrosion resistance in a variety of acidic, alkaline and neutral media (Namboodhiri, 1984). Most of these amorphous alloys are, however, susceptible to environment-assisted fracture processes like hydrogen embrittlement, stress corrosion cracking and liquid metal embrittlement (Namboodhiri and others, 1983). The commercially attractive soft magnetic metallic glasses do not contain chromium, and hence their

corrosion resistance properties are also poor. This work forms part of an effort in evaluating the environment assisted fracture behaviour of commercial metallic glasses so that means of improving their service life could be found.

EXPERIMENTAL METHODS

Three melt-spun metallic glasses were used for this study. Two of them were commercial soft magnetic alloys with no chromium, while the third one was an experimental alloy containing 12% chromium. Their chemical compositions, dimensions and suppliers are listed in Table 1. Environment assisted fracture of these materials was determined using either an Instron universal testing machine or a Hounsfield tensometer. Constant strain-rate tensile tests were performed on smooth ribbons immersed in the corrodent. Strain rates of 10^{-6} to 10^{-3} S^{-1} were employed. The corrodents used were H_2SO_4, HCl, and acidified sodium chloride. A constant D.C. power source and a platinum wire counter electrode were used to pass constant anodic or cathodic currents through the specimen. Environmental variables investigated were the corrodent concentration and the applied anodic or cathodic current density. Fracture surfaces were examined using a scanning electron microscope.

RESULTS AND DISCUSSION

Stress Corrosion Cracking

Stress corrosion cracking susceptibility of the three metallic glasses was evaluated by slow strain-rate tensile tests on specimens exposed to the corrodents either at corrosion potentials or under impressed anodic currents. Figure 1 shows the

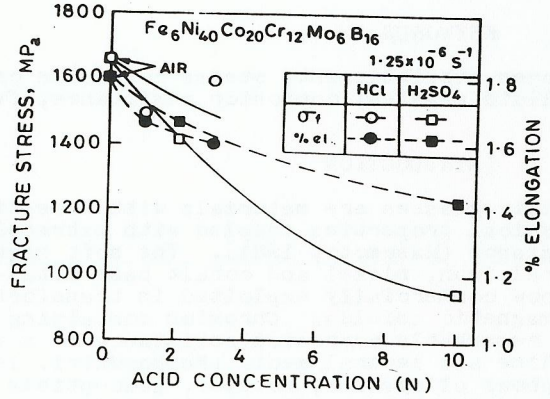

Fig. 1. Effect of acid concentration on the fracture stress and % elongation of $Fe_6Ni_{40}Co_{20}Cr_{12}Mo_6B_{16}$ alloy. Exposure at corrosion potentials.

effect of acid concentration on the fracture stress and percentage elongation of $Fe_6Ni_{40}Co_{20}Cr_{12}Mo_6B_{16}$ alloy exposed at corrosion potentials. Both the strength and the ductility of the alloy are seen to decrease with increasing normality of H_2SO_4 and HCl. The alloy, because of its chromium content is extremely corrosion resistant and showed only a small fraction of one percent of weight loss for exposure times corresponding to those involved in the tensile tests (Namboodhiri, 1983a).

A series of tensile tests were carried out on the FeNiCoCrMoB alloy in a solution of 5N H_2SO_4 + 0.5N NaCl at strain rates varying from 10^{-6} S^{-1} to 10^{-3} S^{-1}. No consistent variation of fracture stress with strain rate could be observed in these tests, but the corrodent reduced the average fracture stress of the alloy by about 10% from the air test value. Previous workers (Kawashima, Hashimoto, and Masumoto, 1976) had shown that an FeNiCrPC amorphous alloy tested in the same corrodent experienced severe reduction in fracture stress at strain rates below 10^{-4} S^{-1}, which was taken as an indication of a hydrogen embrittlement mechanism for the stress corrosion cracking of their alloy.

Stress corrosion cracking susceptibility of the three alloys was also evaluated by applying anodic currents to the specimen during slow strain-rate tensile tests in 0.1N H_2SO_4. The results obtained are shown in Fig. 2. It is seen that only

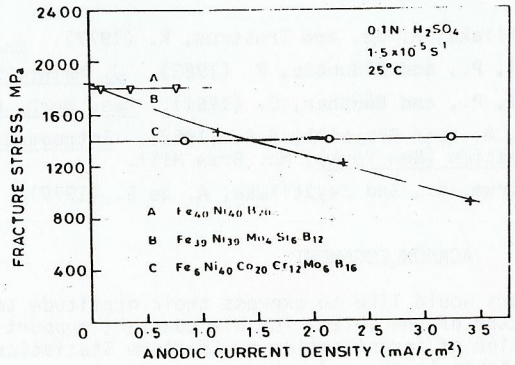

Fig. 2. Effect of anodic currents on the fracture stress.

$Fe_{39}Ni_{39}Mo_4Si_6B_{12}$ alloy is susceptible to loss in fracture stress as the anodic current density increases. Both the other two alloys showed no decrease in fracture stress with impressed anodic currents suggesting that they may not be susceptible to anodic dissolution controlled stress corrosion cracking in this medium. Figure 3 shows the change in fracture morphology

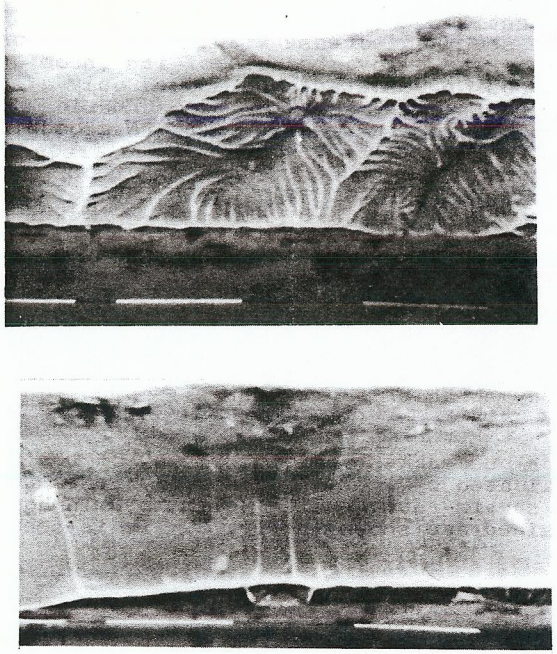

(a)

(b)

Fig. 3. Changes in fracture morphology due to stress corrosion cracking in $Fe_{39}Ni_{39}Mo_4Si_6B_{12}$.

(a) Ductile fracture of specimen tested in air.

(b) Tensile tested in 0.1N H_2SO_4 at a strain rate of 1.5×10^{-5} S^{-1}. Anodic current density = 3.42 mA/cm^2.

induced by stress corrosion cracking in the FeNiMoSiB alloy. While the normal ductile failure of metallic glasses give a typical vein pattern as in Fig. 3(a), the stress corrosion cracking of this alloy results in a very flat and featureless fracture surface (Fig. 3(b)). Even at high magnifications the flat surface remained almost featureless, except for a mottling effect. This featureless, flat fracture surface, normal to the tensile axis, was produced at an applied stress level only half the regular fracture stress of the material. It is to be pointed out here that the tested specimens exhibited several corrosion pits of various sizes on their surface, and probably these pits acted as nucleating sites for brittle cracking in this alloy (Namboodhiri and others, 1983). Potentiostatic polarization measurements showed that this alloy has maximum tendency for pitting.

Hydrogen Embrittlement

The hydrogen embrittlement susceptibility of the three metallic glasses was more thoroughly investigated in this work. Constant strain rate tensile tests at a strain rate of 1.5×10^{-5} S^{-1} were carried out on 60 mm long ribbon specimens. Cathodic currents of various magnitudes were passed through the specimens to introduce different amounts of hydrogen into them (Kawashima, Hashimoto and Masumoto, 1976). Cathodic charging of hydrogen was started 30 minutes before the beginning of the tensile test and continued throughout the test.

Figure 4 shows the effect of cathodic charging on the tensile stress-strain curves of the three metallic glasses. The slopes of the nearly straight line stress-strain curves are not altered by cathodic charging, but the fracture stress decreases drastically with increase in the cathodic current density. This is a

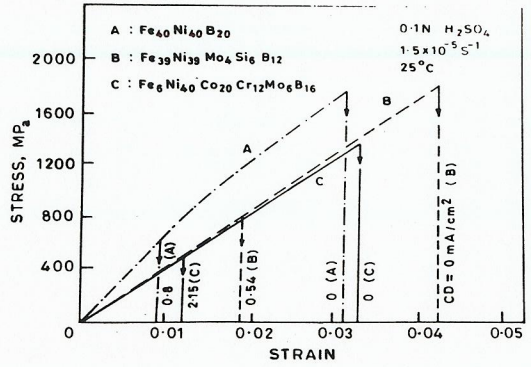

Fig. 4. Effect of cathodic currents on the tensile stress-strain curves of the three metallic glasses. The dotted lines indicate fracture at the given cathodic current density.

behaviour typical of hydrogen embrittled high strength steels and other materials (Nanis and Namboodhiri, 1977). Figure 5 indicates the changes in the fracture stress of these alloys with increasing cathodic current densities. The fracture stress drops to less than half its normal value at cathodic current densities below 0.5 mA/cm^2. Increasing the charging current densities further has only minor effects on the fracture stress. From Fig. 5 it may be inferred that there exists a threshold stress level of about 30 to 50% of the fracture stress in uncharged material below which hydrogen-induced failures do not occur.

Hydrogen causes spectacular changes in the fracture morphology

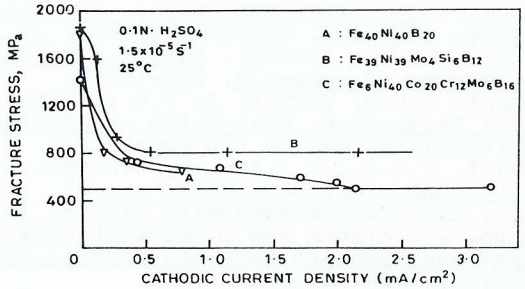

Fig. 5. Change in the fracture stresses of the three alloys with increasing cathodic current density.

of these metallic glasses. Figure 6 shows the ductile fracture surface of $Fe_{40}Ni_{40}B_{20}$. A typical ridge or vein pattern is seen

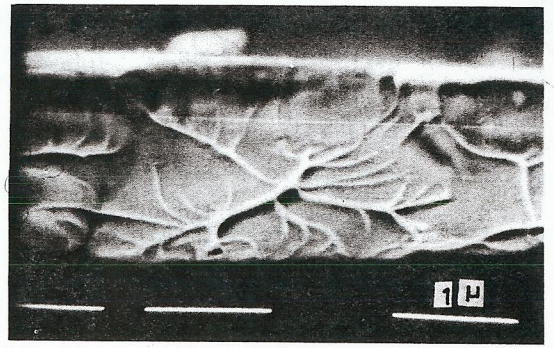

Fig. 6. Typical vein pattern seen on the ductile fracture surface of $Fe_{40}Ni_{40}B_{20}$.

on a very smooth background. The fracture surface, in tensile tested smooth ribbons, is generally inclined at an angle of 45° to the tensile axis and the thickness vector and coincides with the intensely localized shear bands (Davis, 1978). The mechanism of formation of these ridges have been discussed in great detail by many workers (Namboodhiri, 1983b) and is believed to involve the nucleation, stable growth and fast coalescence of shear disk cracks probably attended by local incipient melting

just prior to fracture (Takayama and Maddin, 1976). The incipient melting and sudden cooling of the molten material probably gives rise to a tenacious surface film which gives the smooth appearance to the background (Namboodhiri and others, 1983), and rounds off the top edges of the ridges as seen in Fig. 6.

Figure 7 shows the fracture morphology in hydrogen-charged metallic glasses. A flat fracture surface containing a smooth fracture origin, a fine cellular region and an area of coarse chevrons is seen in this case. Such a three-stage fracture morphology originates from increasing crack growth velocities and crack plane deviation as the brittle crack propagates in the material (Namboodhiri and others, 1983). Cracks generally originate from points near the ribbon surface, and faint cleavage-like steps radiate from the smooth crack origin. The adjacent cellular region has a 'frothy' appearance due to the emergence of a large number of 45° slant shear planes. The coarse chevrons have their apices pointing towards the crack origin, and are made up of a saw-tooth arrangement of shear planes (Davis, 1978). This specimen, which failed at less than half its normal fracture stress, shows considerable localized deformation as evidenced by the profusion of veins or ridges decorating the slant shear planes. A large number of spherical or ellipsoidal holes or microvoids is also seen adjacent to the shear planes in Fig. 7. The highly localized shear bands in metallic glasses are sites of excess free volume where hydrogen may collect and cause void formation (Namboodhiri and others, 1983). Blocked shear bands in crystalline materials like titanium are known (Hack and Leverant, 1982) to cause local hydrogen concentration. The voids seen in Fig. 7 may have formed by the accumulation of molecular hydrogen at the shear bands.

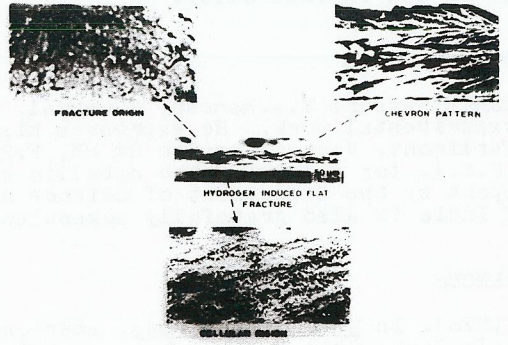

Fig. 7. Fracture morphology in hydrogen charged $Fe_{39}Ni_{39}Mo_4Si_6B_{12}$. Specimen cathodically charged from 0.1N H_2SO_4 at 0.54 mA/cm^2 for 30 minutes and fractured by slow-strain rate tensile test.

CONCLUSIONS

As was shown by several earlier workers, this study also shows that metal-metalloid glasses based on iron and nickel are susceptible to hydrogen embrittlement. Even the highly corrosion resistant Cr-containing alloys are not immune. The major conclusions from this work may be listed as;

i) Hydrogen reduces the fracture stress of the three metallic glasses without altering the slope of the stress-strain curve. A threshold stress level of 30 to 40% of the fracture stress of the uncharged material was found from constant strain rate tensile tests.

ii) Hydrogen significantly alters the fracture morphology of these materials. The slant fracture showing vein patterns obtained in the uncharged material is replaced by a flat brittle fracture surface with three distinct regions. Cleavage steps and Chevron patterns typical of brittle cleavage fracture are seen on hydrogen embrittled fracture surfaces. Localized ductile deformation takes place even under these conditions.

iii) Hydrogen may concentrate at the intensely localized shear bands and form microvoids which may aid the fracture of the material prematurely.

iv) One of the three metallic glasses investigated, namely, $Fe_{39}Ni_{39}Mo_4Si_6B_{12}$ was found to be susceptible to stress corrosion cracking in 0.1N H_2SO_4 under anodic impressed currents. Reduction in fracture stress and a brittle mode of fracture were observed in this alloy under SCC conditions. Many corrosion pits were formed on the surface of the specimen and the pitting susceptibility of this alloy was confirmed by potentiostatic polarization studies. These corrosion pits could act as crack nucleating sites or act as regions where hydrogen generation and ingress to the material may occur. Further study is needed to confirm the mechanism of SCC in this alloy.

ACKNOWLEDGEMENTS

The author thanks Messers T.A.Ramesh, S.Sehgal, and G.Singh for help in the experimental work. He expresses his gratitude to Professor H.Warlimont, Vacuumschmelze Gm bH, F.R.G., and Allied Corporation, U.S.A. for supplying the metallic glass ribbons. Financial support by the Department of Science and Technology, Government of India is also gratefully acknowledged.

REFERENCES

Davis, L.A. (1978). In Metallic Glasses, American Society for Metals, Metals Park, Ohio, Chap. 8 , pp.190-223.

Hack, J.E., and G.R.Leverant (1982). Metall.Trans., 13A, 1729-1738.

Kawashima, A., K.Hashimoto, and T.Masumoto (1976). Corros.Sci., 16, 935-943.

Masumoto, T. (1982). In T.Masumoto and K.Suzuki (Eds.), Proc. 4th Int.Conf. on Rapidly Quenched Metals, Vol.I, Japan Inst. Metals, Sendai, pp.5-10.

Namboodhiri, T.K.G. (1983a). In B.J.Berkowitz and R.O.Scattergood (Eds.) Chemistry and Physics of Rapidly Solidified Materials, TMS/AIME, Warrendale, Pa., pp.197-209.

Namboodhiri, T.K.G. (1983b). Bulletin of the Electron Microscope Society of India, 7, 101-106.

Namboodhiri, T.K.G. (1984). In T.R.Anantharaman (Ed.), Metallic Glasses: Production, Properties and Applications, Trans.Tech. SA, Switzerland, Chap.8 (In Press).

Namboodhiri, T.K.G., T.A.Ramesh, G.Singh, and S.Sehgal (1983). Mater.Sci.Eng., 61, 23-29.

Nanis, L., and T.K.G.Namboodhiri (1977). In R.W.Staehle, J. Hochmann, J.E.Slater and D.McCright (Eds.), Stress Corrosion Cracking and Hydrogen Embrittlement of Iron Base Alloys, NACE, Houston, pp.432-444.

Takayama, S., and R.Maddin (1976). Mater.Sci.Eng., 23, 261-265.

TABLE 1 Experimental Alloys

Alloy	Composition (at.%)	Dimensions Width (mm)	Dimensions Thickness (mm)	Supplier
VITROVAC 0040	$Fe_{40}Ni_{40}B_{20}$	2.5	0.025	Vacuum-Schmelze Gm bH, F.R.G.
VITROVAC 4040	$Fe_{39}Ni_{39}Mo_4Si_6B_{12}$	3.2	0.040	-Do-
Ni-Co alloy	$Fe_6Ni_{40}Co_{20}Cr_{12}Mo_6B_{16}$	4.0	0.040	Allied Corporation, U.S.A.